A Mathematical Model of Surface Electromyographic Measurements

Eike Petersen

***Abstract*—This article describes a detailed, analytical model of the physiological processes involved in the generation and measurement of single muscle fiber action potentials. The model comprises the propagation of an intracellular action potential along a muscle fiber, the diffusion of the resulting electric field throughout the surrounding biological tissues, and the influence of the measurement system. It has been proposed previously; here, an alternative formulation of some parts of the model is proposed and several mathematical properties of the model are remarked that are of interest for a numerical implementation. Results of a numerical simulation highlight the model's capability to reproduce many physiological effects observed in experimental measurements, and to produce realistic test data that may be useful for the validation of signal processing algorithms.**

***Index Terms*—surface electromyography, mathematical modelling, numerical simulation**

I. Introduction

Electromyography (EMG) denotes the measurement of the electrical fields generated by the electrophysiological processes that lead to muscle fiber contraction. EMG is highly relevant for a number of clinical and scientific application fields, since it enables monitoring and analyzing a wide range of physiological parameters that would otherwise be inaccessible. For more background information on EMG, its analysis and many of its applications, refer to, e.g., Merletti and Parker [1].

Mathematical models of surface electromyography (sEMG) are highly useful, on the one hand to advance understanding of the underlying physiological processes, and on the other hand to analyze parameter sensitivities of sEMG measurements and to test and validate sEMG signal processing algorithms.

Over the past decades, researchers have pursued a number of different approaches for the modelling and simulation of different aspects of sEMG measurements. Phenomenological [2, 3, 4] as well as physiological [5, 6, 7, 8, 9, 10, 11] models have been proposed and analyzed. Overviews can be found in Merletti and Parker [1], McGill [2], Stegeman et al. [12] and Rodriguez-Falces et al. [13]. Particular emphasis has been placed on modelling the electric signal produced by a single contraction of a single muscle fiber, the so-called single fiber action potential (SFAP). Classically, simplified dipole, tripole or quadrupole models have been employed for modelling the propagation of the action potential along a contracting muscle fiber [1, 14, 15]. A more precise, continuous model has been proposed by Dimitrov and Dimitrova [9]. This model has been successfully employed, modified and combined with various other models for the remaining physiological processes in a number of publications [5, 6, 8, 16].

Eike Petersen is with the Institute for Electrical Engineering in Medicine, Universität zu Lübeck, 23562 Lübeck, Germany, e-mail: eike.petersen@uni-luebeck.de.

In the following section, the main components of the mathematical model first proposed by Dimitrov and Dimitrova [9] are presented in all brevity. An alternative formulation of an essential part of the model is proposed, and several remarks on the mathematical properties of the model are made. Results of a numerical simulation of the model are presented in section III and are assessed with respect to their physiological credibility. Finally, section IV concludes the article by a brief summary.

II. Mathematical Model

A. Intra-Fiber Action Potential Propagation

The propagation of an intracellular action potential (IAP) from the neuromuscular junction (NMJ) of a muscle fiber along both directions towards the two fiber ends can be modelled by representing the actively firing fiber by a distributed current source and sink. In the model originally proposed by Dimitrov and Dimitrova [9], this distributed current source $\hat{\imath}(z,t)$ is composed of two propagating wave fronts and localized contributions at the NMJ and the two fiber ends. These localized contributions model the IAP generation and extinction process. In the formulation of Farina and Merletti [5], the model reads

$$\hat{\imath}(z,t) = \frac{\mathrm{d}}{\mathrm{d}z}\left[\psi(z - z_i - vt)\, p_1(z) - \psi(-z + z_i - vt)\, p_2(z)\right], \tag{1}$$

where z denotes the spatial variable along the muscle fiber, z_i the location of the NMJ, and p_1 and p_2 are the characteristic functions of the two fiber halves, given by

$$p_1(z) = H(z - z_i) - H(z - z_i - L_1) \tag{2}$$

with the Heaviside step function $H(z)$, $p_2(z)$ analogously. L_1 and L_2 are the distances between the innervation zone and the right and left tendon, respectively, and v denotes the IAP's propagation velocity. Moreover,

$$\psi(z) = \frac{\mathrm{d}}{\mathrm{d}z} V_m(-z), \tag{3}$$

where the function $V_m(z)$ prescribes a model for the trans-fiber membrane voltage wave shape and can be chosen arbitrarily to match simulated or measured data. Refer to Plonsey and Barr [15] for details on the significance of $V_m(z)$.

We could show that formulation (1) is equivalent to choosing

$$\begin{aligned}\hat{\imath}(z,t) = {} & GEN(t)\,\delta(z - z_i) \\ & + \psi'(z - z_i - vt)\, p_1(z) + EOF_1(t)\,\delta(z - z_i - L_1) \\ & + \psi'(-z + z_i - vt)\, p_2(z) + EOF_2(t)\,\delta(z - z_i + L_2),\end{aligned} \tag{4}$$

with the Dirac distribution δ, and

$$EOF_1(t) = -\psi(L_1 - vt), \tag{5}$$

$$EOF_2(t) = -\psi(L_2 - vt), \tag{6}$$

and

$$GEN(t) = 2\,\psi(-vt). \tag{7}$$

This formulation renders – to the author's opinion – the structure of the model more obvious, by clearly distinguishing between propagating and non-propagating signal components, and by revealing the non-smoothness of the resulting distributed current source. Interestingly, one can also show that definitions (5) to (7) are the unique choice for $EOF_1(t)$, $EOF_2(t)$ and $GEN(t)$ that ensures

$$\int_{-\infty}^{\infty} i(z,t)\,\mathrm{d}z = 0 \quad \forall\, t, \tag{8}$$

which means that the fiber does not represent a net current source or sink at any point in time.[1]

B. Electrical Fields in Layers of Biological Tissues

Biological tissues are volume conductors. The existence of an electric field implies the existence of electric currents travelling through the tissue, and vice versa.[2] Due to the comparably low rate of change of physiological systems, it is justified [15] to assume these time-varying electric fields to behave as if they were static at each instant of time, whence they are called *quasi-static*. This assumption amounts to a neglection of the capacitive properties of the tissues. Accordingly, as for static fields, the electric field in a physiological volume conductor is considered equal to the negative gradient of a scalar potential φ, namely,

$$\vec{E} = -\nabla\varphi. \tag{9}$$

By Ohm's law, the current density (current per unit of cross-sectional area) in a volume conductor is proportional to the electric field, that is,

$$\vec{J} = \sigma\vec{E} = -\sigma\nabla\varphi, \tag{10}$$

where σ denotes the conductivity of the medium. Defining a distributed current density source I throughout the region of interest, the divergence of the current density is constrained by

$$\nabla \cdot \vec{J} = I. \tag{11}$$

Combining equations (10) and (11) and assuming a homogeneous, isotropic medium yields Poisson's equation for the diffusion of the potential, namely,

$$\Delta\varphi = -\frac{I}{\sigma}. \tag{12}$$

[1]This assumption is well motivated by physiology. It is also in accordance with the predictions of the reknown Hodgkin-Huxley model for action potential propagation [17].

[2]Note that in biological tissues, the charge carriors are ions, as opposed to electrons in electric wires [15, p. 25].

In the following, the electric field generated by point sources in planar tissue layers will be considered. The muscle layer is assumed to be infinitely extended and planar, and to be covered by an infinitely extended planar layer of fat and an infinitely extended planar layer of skin. Muscle tissue is considered anisotropic in order to reflect the difference in conductivity between currents along the muscle fiber axis and currents across the muscle fiber axis, whereas fat and skin tissue are considered isotropic. Muscle fibers are assumed to run along the z direction, with the x and z dimensions spanning the skin plane, and the y dimension being orthogonal to the skin plane, positive vectors pointing outwards.

The geometrical set-up described above has been analyzed by Farina and Rainoldi [18]. For a point source of strength $\hat{I}$ located at $(0, y_0, 0)$, the authors derive the 2-D spatial Fourier transform of the resulting potential distribution at the skin surface to be

$$\Phi(\hat{I}, k_x, k_z; y_0) = \frac{2\hat{I}}{\sigma_{m,p}} e^{-k_{ya}|y_0|} \cdot \frac{1}{(1+r_c)\,\cosh\!\left(k_y^+\right)\nu\!\left(k_y^+\right) + (1-r_c)\,\cosh\!\left(k_y^-\right)\nu\!\left(k_y^-\right)}, \tag{13}$$

with the abbreviations

$$k_y^+ = k_y(d_f + d_s), \qquad k_y^- = k_y(d_f - d_s), \tag{14}$$

$$k_y = \sqrt{k_x^2 + k_z^2}, \qquad k_{ya} = \sqrt{k_x^2 + r_a k_z^2} \tag{15}$$

and

$$\nu(s) = k_{ya} + s r_m \tanh(s), \tag{16}$$

where $k_x = 2\pi f_x$ and $k_z = 2\pi f_z$ denote the spatial angular frequencies in the x and z directions, respectively. The coefficients

$$r_c = \frac{\sigma_s}{\sigma_f}, \qquad r_m = \frac{\sigma_f}{\sigma_{m,p}}, \qquad \text{and} \qquad r_a = \frac{\sigma_{m,f}}{\sigma_{m,p}} \tag{17}$$

specify ratios of the different tissue conductivities. Finally, y_0 denotes the depth of the point source in the muscle tissue, d_f the thickness of the fat layer and d_s the thickness of the skin layer.

Equation (13) directly yields an analytic description of the 2-D spatial transfer function of the volume conductor *via*

$$H_{\mathrm{vc}}(k_x, k_z; y_0) = \frac{1}{\hat{I}} \cdot \Phi(\hat{I}, k_x, k_z; y_0). \tag{18}$$

We could show that this transfer function describes a spatial low-pass filter, i.e., H_{vc} is a strictly positive function in k_x and k_z with

$$\lim_{k_x \to \pm\infty} H_{\mathrm{vc}}(k_x, k_z^*; y_0) = \lim_{k_z \to \pm\infty} H_{\mathrm{vc}}(k_x^*, k_z; y_0) = 0 \quad \forall\, k_x^*, k_z^* \in \mathbb{R} \tag{19}$$

for any set of positive, finite parameter values and $y_0 \in \mathbb{R}^+$.

C. Surface Electrodes and Their Geometrical Arrangements

EMG measurements are usually taken differentially between a set of electrodes. Consider a regular grid of $r \times s$ electrodes with interelectrode distances d_x and d_z, respectively, where $r = r_a + r_b + 1$ and $s = s_a + s_b + 1$. The variables subscripted by a and b denote the number of electrodes on the two sides of an arbitrarily chosen reference electrode. The grid is assumed to be aligned parallel to the z axis. Assigning weights a_{mn} to the electrodes and assuming all electrodes to attain the same transfer function, the (spatial) transfer function associated to such an electrode configuration is given by [5]

$$H_{\text{ec}}(k_x, k_z) = \sum_{m=-r_a}^{r_b} \sum_{n=-s_a}^{s_b} a_{mn} e^{-jk_x m d_x} e^{-jk_z n d_z}. \quad (20)$$

For the transfer function of a single electrode, arbitrary model assumptions can be made. For details, refer to, e.g., Merletti and Parker [1].

D. Combining the Model Components

Concatenating the spatial transfer functions H_{vc} of the volume conductor, H_{ec} of the electrode configuration and H_{ele} of the electrodes themselves, the global transfer function of the combined system emerges as

$$H_{\text{glo}}(k_x, k_z; y) = H_{\text{vc}}(k_x, k_z; y) \cdot H_{\text{ele}}(k_x, k_z) \cdot H_{\text{ec}}(k_x, k_z). \quad (21)$$

From this, the 2-D potential distribution on the skin surface can be calculated as

$$\varphi(x, z, t) = \int_{\mathbb{R}} \left(i(x, y, z, t) \underset{(x,z)}{*} h_{\text{glo}}(x, z; y) \right) \mathrm{d}y$$

$$= \int_{\mathbb{R}} \mathcal{F}_z^{-1} \left\{ \mathcal{F}_x^{-1} \{ i(k_x, y, k_z, t) \cdot H_{\text{glo}}(k_x, k_z; y) \} \right\} \mathrm{d}y \quad (22)$$

where $i(k_x, y, k_z, t) = \mathcal{F}_x\{\mathcal{F}_z\{i(x, y, z, t)\}\}$ is the 2-D Fourier transform of the current density source $i(x, y, z, t)$, and $*_{(x,z)}$ denotes 2-dimensional convolution in the x and z variables. For a particular electrode location on the skin surface and muscle fibers following straight lines parallel to the skin surface, equation (22) can be evaluated efficiently [5]. We could prove that in this case the integration kernel only has removable singularities, which ensures the convergence of a numerical integration scheme.

III. Simulation Results

A. Single Fiber Action Potentials

Figure 1 shows the simulated SFAPs evoked by two firing muscle fibers (one deeper than the other) as detected at four positions along the fiber. Note how the end-of-fiber artifacts (peaks evoked when either IAP reaches the corresponding tendon) are damped much less by the volume conductor than the propagating signal components (compare upper and lower figure, where due to the fiber lying deeper, the influence of the volume conductor is increased).[3] This behavior is due to the spatial low-pass behavior of the volume conductior – see above – and the end-of-fiber artifacts' low spatial frequency. This discrepany in the damping of the different signal components is the reason why electrical crosstalk from adjacent muscles is mainly caused by end-of-fiber signals [1, 19].

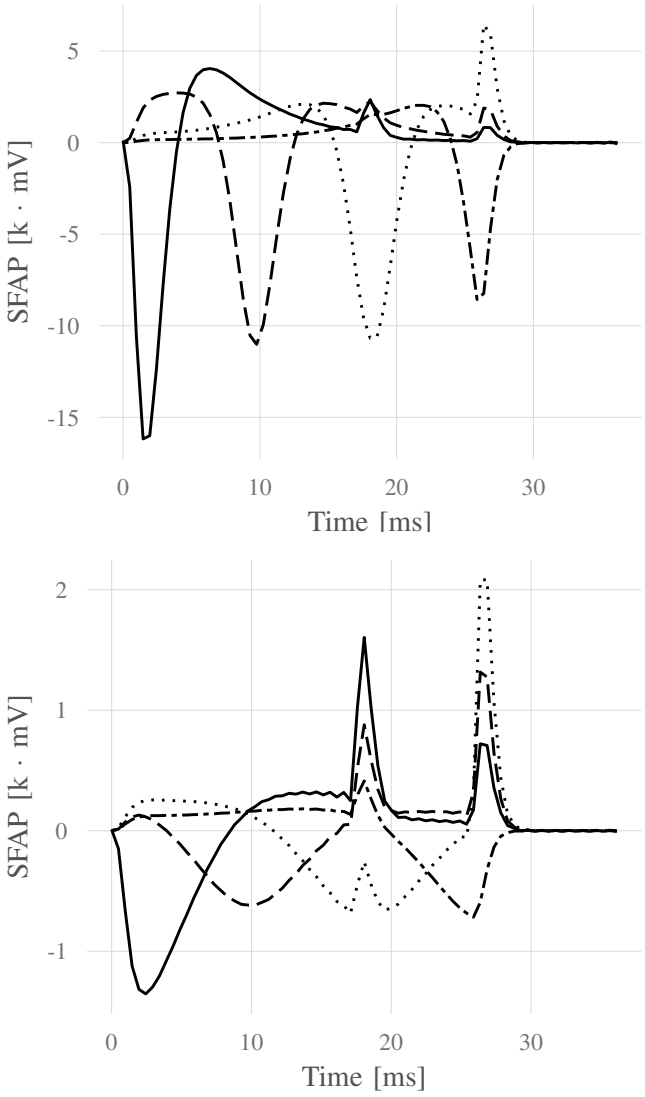

Fig. 1: Upper figure: simulated single fiber action potentials (SFAPs) evoked by a single firing muscle fiber as detected by four surface electrodes positioned above the NMJ (solid), above one of the two fiber ends (dash-dotted), and at two positions in between (dashed, dotted). Lower figure: same as upper, but for a deeper fiber.

B. Macroscopic Signal Properties

A constant-force (non-fatiguing) contraction of a muscle consisting of about 26 000 fibers has been simulated. Figure 2 shows the Fourier spectrum of the resulting signal,

[3] The additional end-of-fiber signal at around 18 ms is due to the two fiber halves being of different lengths - at that point in time, the wave front travelling along the opposite direction from the NMJ has reached the other fiber end.

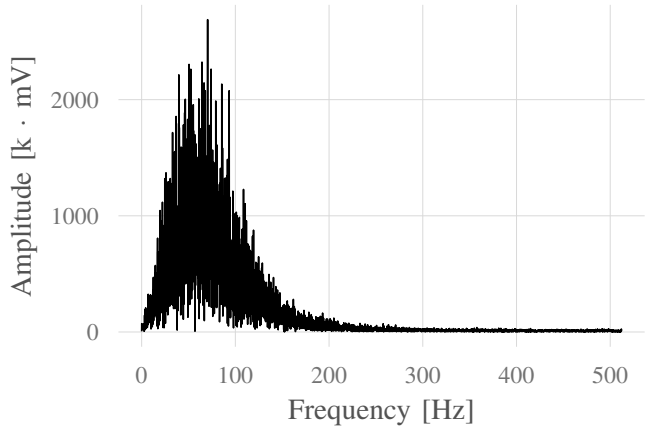

Fig. 2: Fourier spectrum of a simulated, differentially detected sEMG measurement.

which closely resembles spectra found for real measurements. Interestingly, the simulated signal exhibits a purely Gaussian amplitude distribution, whereas measured data seem to attain an amplitude distribution somewhere between Gaussian and Laplacian [20]. The cause of this discrepancy between simulation and reality is currently unknown.

IV. Conclusion

In this short article, a previously described model for the generation and measurement of electromyographic signals has been recapitulated. The model is composed of a current source model of an actively firing muscle fiber and of spatial transfer functions of the surrounding biological tissues and the detection system. An alternative formulation of the IAP generation, propagation and extinction model component has been proposed; several mathematical properties of the model have been remarked. A numerical simulation has shown that the model qualitatively reproduces many of the features of real sEMG measurements. It is hence deemed useful for the analysis of parameter sensitivities and interactions and for the validation of sEMG signal processing algorithms.

References

[1] R. Merletti and P. A. Parker, Eds., *Electromyography*. John Wiley & Sons, Inc., 2004.

[2] K. C. McGill, "Surface electromyogram signal modelling," *Med. Biol. Eng. Comput.*, 2004.

[3] N. Hogan and R. W. Mann, "Myoelectric signal processing: Optimal estimation applied to electromyography - part I: Derivation of the optimal myoprocessor," *IEEE T. Bio.-Med. Eng.*, vol. 27, no. 7, pp. 382–395, Jul. 1980.

[4] C. Sinderby, L. Lindström, and A. E. Grassino, "Automatic assessment of electromyogram quality," *J. Appl. Physiol.*, vol. 79, no. 5, pp. 1803–1815, 1995.

[5] D. Farina and R. Merletti, "A novel approach for precise simulation of the EMG signal detected by surface electrodes," *IEEE T. Bio.-Med. Eng.*, 2001.

[6] D. Farina, L. Mesin, S. Martina, and R. Merletti, "A surface EMG generation model with multilayer cylindrical description of the volume conductor," *IEEE T. Bio.-Med. Eng.*, 2004.

[7] J. L. Dideriksen, D. Farina, M. Baekgaard, and R. M. Enoka, "An integrative model of motor unit activity during sustained submaximal contractions," *J. Appl. Physiol.*, vol. 108, no. 6, pp. 1550–1562, 2010.

[8] J. L. Dideriksen, D. Farina, and R. M. Enoka, "Influence of fatigue on the simulated relation between the amplitude of the surface electromyogram and muscle force," *Phil. Trans. R. Soc. A*, 2010.

[9] G. V. Dimitrov and N. A. Dimitrova, "Precise and fast calculation of the motor unit potentials detected by a point and rectangular plate electrode," *Med. Eng. Phys.*, 1998.

[10] A. J. Fuglevand, D. A. Winter, and A. E. Patla, "Models of recruitment and rate coding organization in motor-unit pools," *J. Neurophysiol.*, vol. 70, no. 6, pp. 2470–2488, 1993.

[11] M. Mordhorst, T. Heidlauf, and O. Röhrle, "Predicting electromyographic signals under realistic conditions using a multiscale chemo–electro–mechanical finite element model," *Interface Foc.*, vol. 5, 2015.

[12] D. F. Stegeman, J. H. Blok, H. J. Hermens, and K. Roeleveld, "Surface EMG models: properties and applications," *J. Electromyogr. Kines.*, vol. 10, pp. 313–326, 2000.

[13] J. Rodriguez-Falces, J. Navallas, and A. Malanda, "EMG modeling," in *Computational Intelligence in Electromyography Analysis - A Perspective on Current Applications and Future Challenges*, G. R. Naik, Ed. InTech, Oct. 2012.

[14] R. Merletti, L. Lo Conte, E. Avignone, and P. Guglielminotti, "Modeling of surface myoelectric signals. I. Model implementation," *IEEE T. Bio.-Med. Eng.*, vol. 46, no. 7, pp. 810–820, Jul. 1999.

[15] R. Plonsey and R. C. Barr, *Bioelectricity*, 3rd ed. Springer, 2007.

[16] W. Wang, A. D. Stefano, and R. Allen, "A simulation model of the surface EMG signal for analysis of muscle activity during the gait cycle," *Comput. Biol. Med.*, vol. 36, pp. 601–618, 2006.

[17] P. H. Kleinpenning, T. H. J. M. Gootzen, A. Van Oosterom, and D. F. Stegeman, "The equivalent source description representing the extinction of an action potential at a muscle fiber ending," *Math. Biosci.*, vol. 101, pp. 41–61, 1990.

[18] D. Farina and A. Rainoldi, "Compensation of the effect of sub-cutaneous tissue layers on surface EMG: a simulation study," *Med. Eng. Phys.*, 1999.

[19] N. A. Dimitrova, G. V. Dimitrov, and O. A. Nikitin, "Neither high-pass filtering nor mathematical differentiation of the EMG signals can considerably reduce cross-talk," *J. Electromyogr. Kines.*, vol. 12, no. 4, pp. 235 – 246, 2002.

[20] E. A. Clancy and N. Hogan, "Probability density of the surface electromyogram and its relation to amplitude detectors," *IEEE T. Bio.-Med. Eng.*, vol. 46, no. 6, pp. 730–739, Jun. 1999.